

Si nanophotonics based cantilever sensor

Chengkuo Lee,^{1,2,a)} Jayaraj Thillaigovindan,¹ Chii-Chang Chen,³ Xian Tong Chen,² Ya-Ting Chao,⁴ Shaohua Tao,² Wenfeng Xiang,¹ Aibin Yu,² Hanhua Feng,² and G. Q. Lo²

¹Department of Electrical and Computer Engineering, National University of Singapore, 4 Engineering Drive 3, Singapore 117576, Singapore

²Institute of Microelectronics (IME), Agency for Science, Technology and Research (A*STAR), 11 Science Park Road, Singapore Science Park II, Singapore 117685, Singapore

³Department of Optics and Photonics, National Central University, Zhong-Li, Taiwan 32001, Republic of China

⁴Department of Computer Sci. and Eng., Yuan Ze University, Chung-Li, Taiwan 32003, Republic of China

(Received 29 June 2008; accepted 10 August 2008; published online 19 September 2008)

We present design and simulation results of a novel nanomechanical sensor using silicon cantilever embedded with a two-dimensional photonic crystal microcavity resonator. Both of resonant wavelength and resonant wavelength shift could be measured as a function of various physical parameters such as applied force, strain, and displacement. Rather linear relationship is derived for strain and resonant wavelength shift. This new nanomechanical sensor shows promising features for biomolecules detection. © 2008 American Institute of Physics. [DOI: 10.1063/1.2987515]

Integration of photonic crystals (PCs) with microelectromechanical systems (MEMS) based structures and function elements renders a new category of nanometer scale devices, i.e., the optical nanoelectromechanical systems (NEMS). One of the major research topics in optical NEMS is optical nanomechanical sensors. According to detected changes in the intrinsic optical properties of PC, the optical nanomechanical sensors measure physical parameters such as force, stress, strain, and displacement. Concept of a displacement sensor comprising two planar PC waveguides aligned along the same axis of light propagation is proposed by Levy *et al.*¹ It deploys the output light intensity as the sensing signals, which are functions of alignment accuracy. A suspended silicon bridge structure integrated with PC waveguide microcavity based optical resonator has been proposed as a nanomechanical sensor.²

Micromachined cantilever based biosensors has been studied for a while.^{3,4} The bending of microcantilever is very sensitive to changes in the environment, more specifically, to changes at the surface of the microcantilever. Available technologies lead to the cantilevers with properly functionalized surface on one side of cantilever surface. Highly selective probe molecules (e.g., oligonucleotides, DNA, and antibody) are immobilized on said surface of cantilever where they typically form a monolayer and can capture the targeted DNA and protein molecules. MEMS based sensing mechanisms of the piezoresistive scheme,⁵ the piezoelectric scheme,^{6,7} and the capacitive scheme⁸ have been demonstrated a decade ago. In this study we proposed a new silicon cantilever integrated with two-dimensional (2D) PC based microcavity resonator. This letter reveals a new sensing mechanism for cantilever deflection. It is a promising nanomechanical sensor for cantilever based biosensing applications.

As shown in Figs. 1(a)–1(c), the proposed novel cantilever embedded with a PC microcavity resonator at the junction edge of cantilever and substrate. The PC structure con-

tains an array of air holes in the silicon cantilever layer of 220 nm with a hexagonal lattice constant of $a=500$ nm and the radius of all holes of $r=180$ nm, where a silicon waveguide is formed by removing one row of air holes in a U-shaped layout [Fig. 1(c)]. The deep UV photolithography and Si deep reactive ion etching can enable the PC cantilever made of silicon device layer of a silicon-on-insulator (SOI) wafer. The free-standing PC cantilever is derived by removing Si and SiO₂ layers underneath Si PC cantilever from the backside of SOI wafer [Fig. 1(b)]. PC device of a pair of two-air hole located along the PC waveguide has been investigated as a good optical microcavity resonator.⁹ In a present study, microcavity resonator of two-hole pairs with a defect length of $A_d=640$ nm is located near the input light terminal of this U-shaped silicon waveguide, where the defect length is defined as the distance between the second hole and the third hole, i.e., the optical resonant cavity length. The defect length of 640 nm is derived as of $2a-2r$. The edge of base silicon substrate is intersecting with free-standing cantilever along the dashed line as shown on Fig. 1(c). The wavelength shift of output optical resonant peak is mainly attributed to change of the defect length of microcavity resonator.² Based on this configuration of PC cantilever, the most significant strain is happened at the region of defect length when cantilever end is under an applied force.

We have considered 15 μm wide cantilevers of three different lengths, i.e., 25, 30 and 50 μm . By using finite element analysis (FEA), we used Young's modulus of 130 GPa and Poisson ratio of 0.3 to derive the strain distribution along this free-standing cantilever structure. Second the 2D finite-difference time-domain (FDTD) method was deployed to simulate the propagation of the electromagnetic waves in the PC waveguides. According to a numerical approach,¹⁰ we derived the effective refractive index as of 2.7967 for the air/Si/air three layers of the white part in Fig. 1(c). This effective refractive index represents the silicon cantilever suspended in air. The circled aread in Fig. 1(c) represents the air holes of PC structures. According to the FEA results of cantilever deformation under various force loads, the position information of deformed shape of holes of PC microcav-

^{a)}Author to whom correspondence should be addressed. Electronic addresses: elelc@nus.edu.sg and leec@ime.a-star.edu.sg.

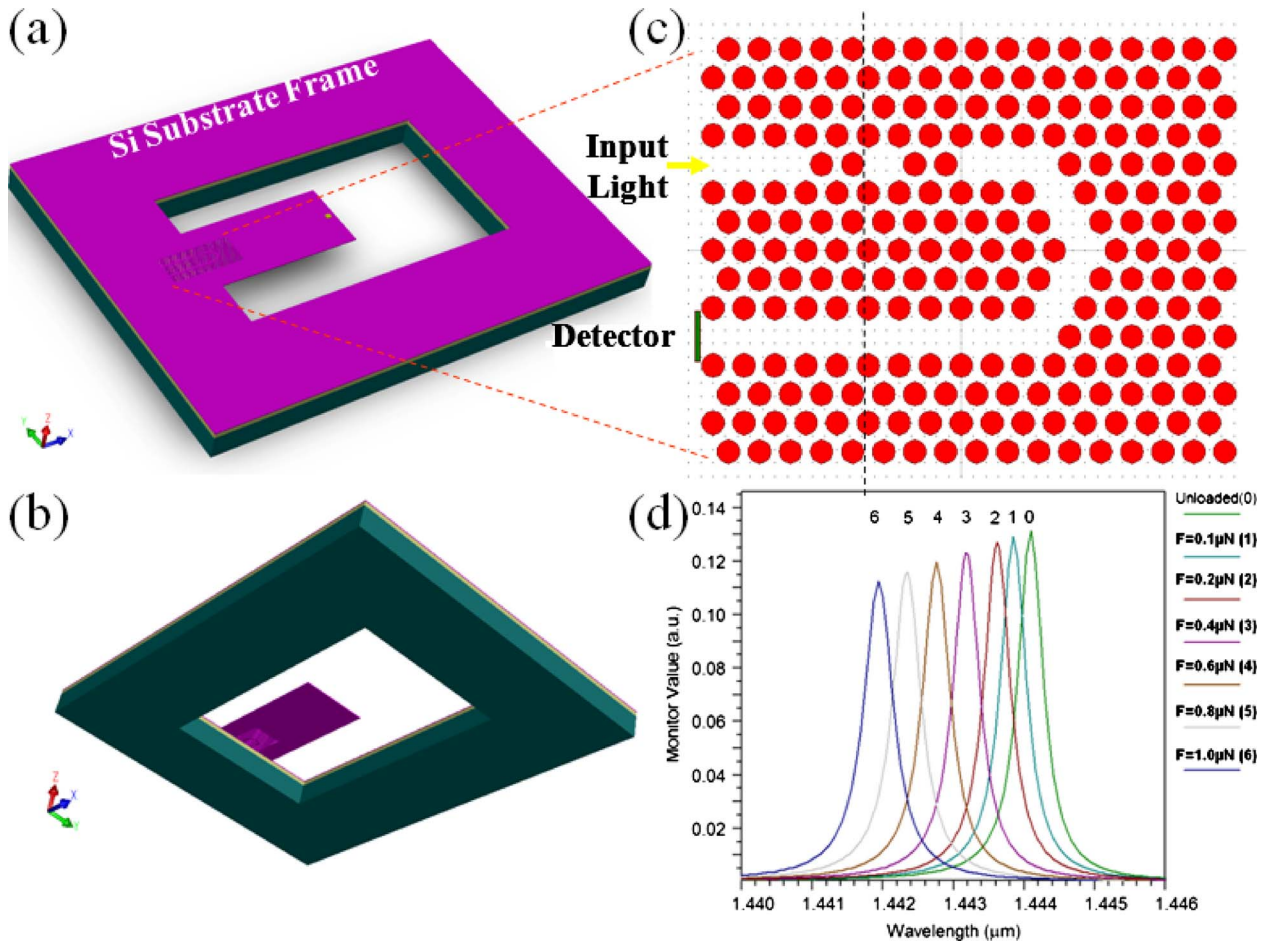


FIG. 1. (Color online) Tilted (a) top view drawing and (b) back side view drawing of PC cantilever. (c) Schematic drawing of PC microcavity resonator on U-shaped Si waveguide. (d) The resonant wavelength peaks of a $50 \mu\text{m}$ cantilever under various force loads.

ity resonator is provided as the revised layout of PC structure in FDTD simulation. Finally, we derived the resonant wavelength shift based on the FDTD simulated output spectrum with respect to cantilever deformation under various force loads. Figure 1(d) shows the simulated resonant wavelength peaks for $50 \mu\text{m}$ long cantilever under various applied force from 0.1 to $1 \mu\text{N}$. The resonant wavelength peak of the unloaded case is simulated as 1444.097 nm . When the force loads increase, the resulting resonant wavelength peak moves to the shorter wavelength region and the observed quality factor of the resonant wavelength peak decreases. The same trend is observed for data derived from cantilevers of 30 and $25 \mu\text{m}$ lengths. It also shows that linear relationship between the resonant wavelength and the force loads.

Combining the results of FEM and FDTD method, the vertical displacements, i.e., the z -displacement, at cantilever end and at right hand side edge of PC are plotted as the function of the detected resonant wavelength shift $\Delta\lambda$ for $50 \mu\text{m}$ cantilever in Fig. 2, where the resonant wavelength shift is defined as the difference between the resonant wavelength of deformed cantilever and the unloaded one. Linear fitting lines are derived for both positions. We can get the same trend and conclusion for plots of cantilevers of 30 and $25 \mu\text{m}$ in length. The vertical displacement at cantilever end and at PC structure end under $1 \mu\text{N}$ is simulated as 20.35 and $1.15 \mu\text{m}$, respectively, while the corresponding resonant wavelength shift is measured as 2.16 nm at $1 \mu\text{N}$ force load. The derived vertical displacement at cantilever end under

$1 \mu\text{N}$ is simulated as 4.79 and $2.82 \mu\text{m}$ for cantilevers of 30 and $25 \mu\text{m}$, respectively.

We have observed and discussed in Ref. 2 that the resonant wavelength shift is strongly dependent on the defect length. Thus we define the strain as a ratio of the change in defect length, i.e., ΔA_d , to the original defect length, A_d . In other words, strain is the percent change in the defect length. The variation in ΔA_d revises the A_d such that the resonant wavelength changes. Figure 3 shows the linear relationship between the absolute value of strain and the resonant wavelength shifts for three kinds of cantilevers. Regarding the 0.1 nm wavelength shift resolution, the detectable smallest strain is derived as 0.0136% , 0.0133% , and 0.0132% for cantilevers of 50 , 30 , and $20 \mu\text{m}$ in length, respectively. Based on

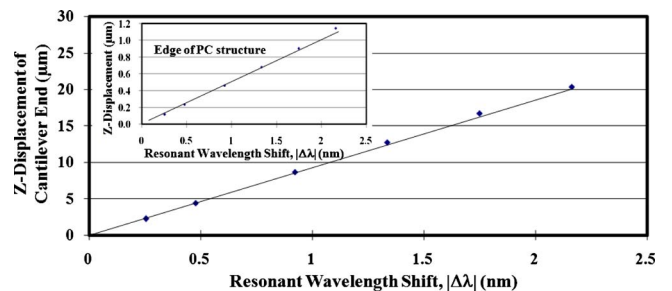


FIG. 2. (Color online) The derived Z -displacement at the end of $50 \mu\text{m}$ cantilever and at the end of right edge of PC structure (inset) vs resonant wavelength shift.

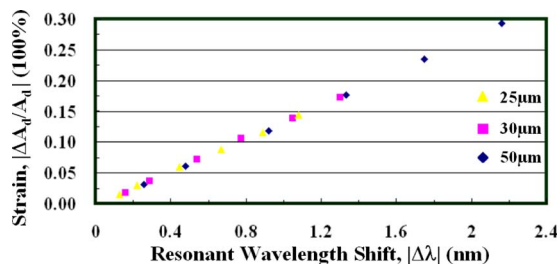


FIG. 3. (Color online) The derived strain vs the resonant wavelength shift for various cantilevers.

Figs. 2 and 3, in the case of the minimum detectable strain, the equivalent vertical deflection at the cantilever end and force load are $0.94 \mu\text{m}$ and $0.046 \mu\text{N}$ for the $50 \mu\text{m}$ cantilever, $0.34 \mu\text{m}$ and $0.071 \mu\text{N}$ for the $30 \mu\text{m}$ cantilever, and $0.26 \mu\text{m}$ and $0.092 \mu\text{N}$ for the $25 \mu\text{m}$ cantilever, respectively. It implies that the longer cantilever is good at measuring smaller force, while the shorter cantilever is good at detecting smaller strain and the minimum detectable vertical deflection of cantilever end, since the longer the cantilever is, the softer it is.

Very interesting linear results are observed for three cantilevers of different lengths in Fig. 3. Svelto¹¹ has described a linear relation between the strain ($\Delta A_d/A_d$) and $\Delta\lambda$ in the Fabry–Pérot based resonator. Additionally, referring to a simple cantilever beam structure, the strain at the surface of the junction edge of cantilever and base substrate is defined by

$$\text{strain} = 6F/Ewt^2,$$

where F is an applied force at cantilever end and E , t , w , and l represent Young's modulus, thickness, width, and length of cantilever, respectively. As a result, either resonant wavelength or resonant wavelength shift could be measured as a function of various physical parameters, such as force load, strain, and displacement.

The authors acknowledge research grants (Grant Nos. R-263-000-475-112 and R-263-000-358-112/133) from the National University of Singapore.

¹O. Levy, B. Z. Steinberg, N. Nathan, and A. Boag, *Appl. Phys. Lett.* **86**, 104102 (2005).

²C. Lee, R. Radhakrishnan, C.-C. Chen, J. Li, J. Thillaigovindan, and N. Balasubramanian, *J. Lightwave Technol.* **26**, 839 (2008).

³N. V. Lavrik, M. J. Sepaniak, and P. G. Datskos, *Rev. Sci. Instrum.* **75**, 2229 (2004).

⁴C. Ziegler, *Anal. Bioanal. Chem.* **379**, 946 (2004).

⁵M. Tortonese, R. C. Barrett, and C. F. Quate, *Appl. Phys. Lett.* **62**, 834 (1993).

⁶T. Itoh, C. Lee, and T. Suga, *Appl. Phys. Lett.* **69**, 2036 (1996).

⁷C. Lee, T. Itoh, R. Maeda, and T. Suga, *Rev. Sci. Instrum.* **68**, 2091 (1997).

⁸J. Brugger, R. A. Buser, and N. F. de Rooij, *J. Micromech. Microeng.* **2**, 218 (1992).

⁹J. S. Foresi, P. R. Villeneuve, J. Ferrera, E. R. Thoen, G. Steinmeyer, S. Fan, J. D. Joannopoulos, L. C. Kimerling, H. I. Smith, and E. P. Ippen, *Nature* **390**, 143 (1997).

¹⁰K. Kawano and T. Kitoh, *Introduction to Optical Waveguide Analysis: Solving Maxwell's Equations and the Schrödinger Equation* (Wiley, New York, 2001), Chap. 2.

¹¹O. Svelto, *Principles of Lasers*, 3rd ed. (Plenum, New York, 1989), Chap. 4, p. 153.